A&A 399, 995–1002 (2003)
DOI: 10.1051/0004-6361:20021856

Astronomy & Astrophysics

Near–infrared and ISOCAM observations of the Chamaeleon II dark cloud⋆,⋆⋆

P. Persi[1], A. R. Marenzi[1], M. Gómez[2], and G. Olofsson[3]

[1] Istituto Astrofisica Spaziale e Fisica Cosmica, CNR, via del Fosso del Cavaliere, 00133, Roma, Italy
e-mail: persi@rm.iasf.cnr.it
[2] Observatorio Astronómico de Córdoba, Laprida 854, 5000 Córdoba, Argentina
[3] Stockholm Observatory, SCFAB, 106 91 Stockholm, Sweden

Received 3 October 2002 / Accepted 3 December 2002

Abstract. An infrared study including ISOCAM images at 6.75 and 14.3 μm of a large portion ($28' \times 26'$) of the Chamaeleon II dark cloud and sub-arcsec resolution JHK_s images of the central ($4.9' \times 4.9'$) area is presented. Combining the ISOCAM observations with J and K_s photometry obtained with DENIS, we have found 12 young stars, of which 8 are previously identified sources. Of the new candidate YSOs, ISO-ChaII13 shows a clear mid–IR excess with an infrared luminosity of ~0.02 $L_\odot$ and a stellar luminosity ≥0.01 $L_\odot$. This last value of luminosity corresponds to that expected for a sub–stellar object with an age between 1–10 Myr. The analysis of the $J - H/H - K$ diagram of the sources detected in the central part of the dark cloud has allowed us to identify 10 very faint sources not found by ISOCAM with possible near-IR excesses that may be embedded young brown dwarfs. Finally, the center of the dark cloud is characterized by the presence of the Class I YSO IRAS 12553–7651 (ISO-ChaII28) with L_{bol} = 1.49 $L_\odot$, and associated with a faint nebulosity observed at 2.2 μm.

Key words. stars: formation – stars: low-mass, brown dwarfs – stars: pre-main sequence – infrared: stars

1. Introduction

Recent large-scale infrared surveys of nearby star forming regions carried out in two broad-band filters, LW2(5–8.5 μm) and LW3(12–18 μm) with the mid-infrared camera ISOCAM (Cesarsky et al. 1996) aboard the ISO satellite (Kessler et al. 1996), have allowed investigators to extend the study of the young stellar population to very low luminosity objects down to $L_\star \sim 0.03\ L_\odot$. New very low luminosity young stellar objects (YSOs) near or below the hydrogen burning limit have been discovered in several regions (see Olofsson et al. 1999 for RCrA; Kaas et al. 1999 for Serpens; Persi et al. 2000 for Chamaeleon I; Bontemps et al. 2001 for ρ Ophiuchi).

The characteristics of these very low-mass YSOs such as the luminosity, the spectral energy distribution class and the spectral type can be derived combining the mid-infrared observations with the high sensitivity photometric JHK images and near-IR spectroscopy. This approach turned out to be a powerful tool to study the low mass population of the Chamaeleon I dark cloud (Persi et al. 1999; Persi et al. 2001; Gómez & Persi 2002). Therefore its application to other nearby clouds can provide some clues to better understand the formation and early evolution of extremely low mass objects.

The dark cloud Chamaeleon II (D = 178 pc, Whittet et al. 1997) is part of the Chamaeleon complex composed at least of six clouds (Boulanger et al. 1998). Several pre-main-sequence (PMS) stars with H_α emission were found in this region by Schwartz (1977) and Hartigan (1993). IRAS data and near-IR photometry allowed Whittet et al. (1991), Prusti et al. (1992), and Larson et al. (1998) to classify most of these objects as classical T Tauri stars. A CO and CS study of the IRAS sources in Cha II (Olmi et al. 1994; Olmi et al. 1997) identified IRAS 12553–7651, located near the center of the region, as a young low luminosity stellar object with a probable molecular outflow. Using the DENIS data, Vuong et al. (2001) obtained an extinction map of the region and, de-reddening the IJK_s detected sources, proposed a list of 51 candidate low-mass T Tauri stars and/or young brown dwarfs. Cha II is probably in an earlier evolutionary stage than Cha I as suggested by Prusti et al. (1992) and by the recent X-ray ROSAT pointed observations reported by Alcalá et al. (2000).

In this paper, we report the results of an infrared study of the Chamaeleon II dark cloud based on ground-based near–IR observations (images and spectroscopy) and mid-IR images taken with ISOCAM. Preliminary results derived from an initial analysis of the latest data were reported by Nordh et al. (1996). In Sect. 2 observational details relative to the ISOCAM and JHK_s images and near-IR spectroscopy are given. In Sect. 3.1 we combine the ISOCAM data with the DENIS

Send offprint requests to: P. Persi, e-mail: persi@rm.iasf.cnr.it

⋆ Based on observations collected at the European Southern Observatory, Chile, ESO proposal N.65.I-0054, CTIO(Chile), and ISOCAM observations N.11500619, and 11500620.

⋆⋆ Tables 1 and 2 are only available in electronic at the CDS via anonymous ftp to cdsarc.u-strasbg.fr (130.79.125.5) or via http://cdsweb.u-strasbg.fr/cgi-bin/qcat?J/A+A/399/995

photometry in order to identify new members of the cloud. We discuss the color–color ($J-H$ vs. $H-K_s$) and the color–magnitude (K_s vs. $H-K_s$) diagrams obtained from sub-arcsec resolution SOFI JHK_s images for the sources lying in the densest part of the cloud (Sect. 3.2). Finally in Sect. 3.2.1 we combine near-IR photometry, ISOCAM flux densities and IRAS data to obtain the spectral energy distribution (SED) of IRAS 12553–7651 and use a spherically symmetric dust envelope model to fit the data. The conclusions are summarized in Sect. 4.

2. Observations and data reduction

2.1. ISOCAM images

A region of approximately $28'\times26'$ of Cha II, centered at $\alpha_{2000} = 13^h00^m47^s$ and $\delta_{2000} = -77°06'09''$, was surveyed with ISOCAM in raster mode at LW2(5–8.5 μm) (TDT N.11500619) and LW3(12–18 μm)(TDT N.11500620). All the frames were observed with a pixel field of view (PFOV) of $6''$, intrinsic integration time $T_{int} = 2.1$ s and ~15 s integration time per sky position. The total integration time was of 4472 s and 4474 s for LW2 and LW3, respectively.

The raw data were reprocessed using the last version of the Cam Interactive Analysis (CIA v5.0) software[1]. We have applied the same procedure as described by Persi et al. (2000) to reduce the images and to obtain the photometry of the detected sources. The detection limits for this survey are about 0.8 mJy (1σ) for LW2 ($\lambda_{eff} = 6.75$ μm) and 1.3 mJy (1σ) for LW3 ($\lambda_{eff} = 14.3$ μm). We have detected a total of 115 sources, of which 112 at 6.75 μm and 35 at 14.3 μm with a S/N ratio ≥3. Approximately 70% of the sources found at 6.75 μm have been identified with visible stars, and in particular 36 with the Guide Star Catalogue (GCS) stars. From a positional comparison between the GSC stars and our sources, we derive a mean astrometric accuracy for the ISOCAM sources of about ±4–5″ in both coordinates. The complete list of the ISOCAM sources including the positions and flux densities is given in Table 1.

2.2. Near-IR images

We obtained J, H, and K_s images of the central part of Cha II covering an area of $4.9'\times4.9'$ with the SOFI near-IR camera at the ESO 3.58 m New Technology Telescope (NTT) on the night of April 28, 2000 under very good seeing conditions (~0.3″). SOFI uses a 1024×1024 pixel HgCdTe array and provides a field of view of $299''\times299''$ with a scale of 0.292″/pix.

The near-IR images were taken in *jitter mode* with 8 single frames each of 60 s exposure and with a jitter width of 40″. The data were flux calibrated by observing the NICMOS faint standard star S064–F from the list of Persson et al. (1998), before and after the observations of Cha II. The procedure used to derive the final co-added images is described in Persi et al. (2001). Stellar photometry of the detected sources was obtained using the DAOPHOT (Stetson 1987) routine within IRAF[2] with an aperture of 1.5″. The astrometry of the images was performed comparing our frames with the Digitized Sky Survey (DSS) plates. We estimated an average uncertainty of the near-IR positions better than 1″. At the sensitivity of 3σ (for point–like sources) $J = 21.4$, $H = 20.0$ and $K_s = 18.9$, we detected 197 sources in K_s, 173 in H, and 103 in J. A complete list of these sources including the photometry and positions is reported in Table 2.

Figure 1 shows the near-IR images of Chamaeleon II. The red source at the center of the images associated with a small nebulosity in K_s is the young object IRAS 12553–7651 (ISO-ChaII28).

2.3. Near-IR spectroscopy

Near-IR spectra of three new candidate young stellar objects in Cha II (ISO–ChaII13, 98, and 110, see next section) were obtained on February 27–28 2002 with the OSIRIS (Ohio State Infrared Imager and Spectrometer) on the CTIO Blanco 4 m telescope. OSIRIS was used in the X-Disp (multi-order/cross-dispersed) mode with the f/2.8 camera and a slit 30″ long and 1.2″ wide. This configuration gives $R\,(\lambda/\Delta\lambda) \sim 1200$ (2 pixels), while covering the J, H, and K bands simultaneously on a 1024×1024 HgCdTe detector at a plate scale of 0.403″.

We obtained 5 spectra per target of 200 s. each, moving the telescope 5″ along the slit between consecutive positions. In addition we observed a G5 V atmospheric standard for telluric absorption corrections taken at similar air-mass. We took multiple flat field images with a dome screen, using incandescent lamps on and off. A He Ne Ar gas-discharge lamp, also taken on and off, provided the wavelength calibration. The data were reduced with the IRAF package. We subtracted one image from another (using pairs of nodded observations) to eliminate the background and sky contribution in first approximation. This subtraction automatically took care of the dark current and bias level. We flat-fielded our data dividing by a normalized dome flat. We used the *echelle* task APALL to trace and extract the spectra along a 10 pixel wide aperture on the co-added images. A further sky subtraction was done by fitting a polynomial to the regions on either side of the aperture.

We removed telluric features dividing the spectra of our sources by the G5 V atmospheric standard spectrum. We used the normalized solar spectrum[3] convolved to the OSIRIS spectral resolution to multiply the telluric corrected spectra. A Planck function at the temperature of the standard (5500 K) reproduced the corresponding telluric stellar continuum. In this way, we recovered the true spectral shape of our sources.

Figure 2 displays the spectra for these three sources. For ISO-ChaII98 and 110 we only show the HK data as the S/N ratio for the J band was rather poor.

[1] The ISOCAM data presented in this paper were analyzed using CIA a joint development by the ESA Astrophysics Division and the ISOCAM Consortium. The ISOCAM Consortium is led by the ISOCAM PI, C. Cesarsky.

[2] IRAF is distributed by the National Optical Astronomy Observatory, which is operated by the Association of Universities for Research in Astronomy, Inc. under contract to the National Science Foundation.

[3] NSO/Kitt Peak FTS data used here were produced by NSF/NOAO.

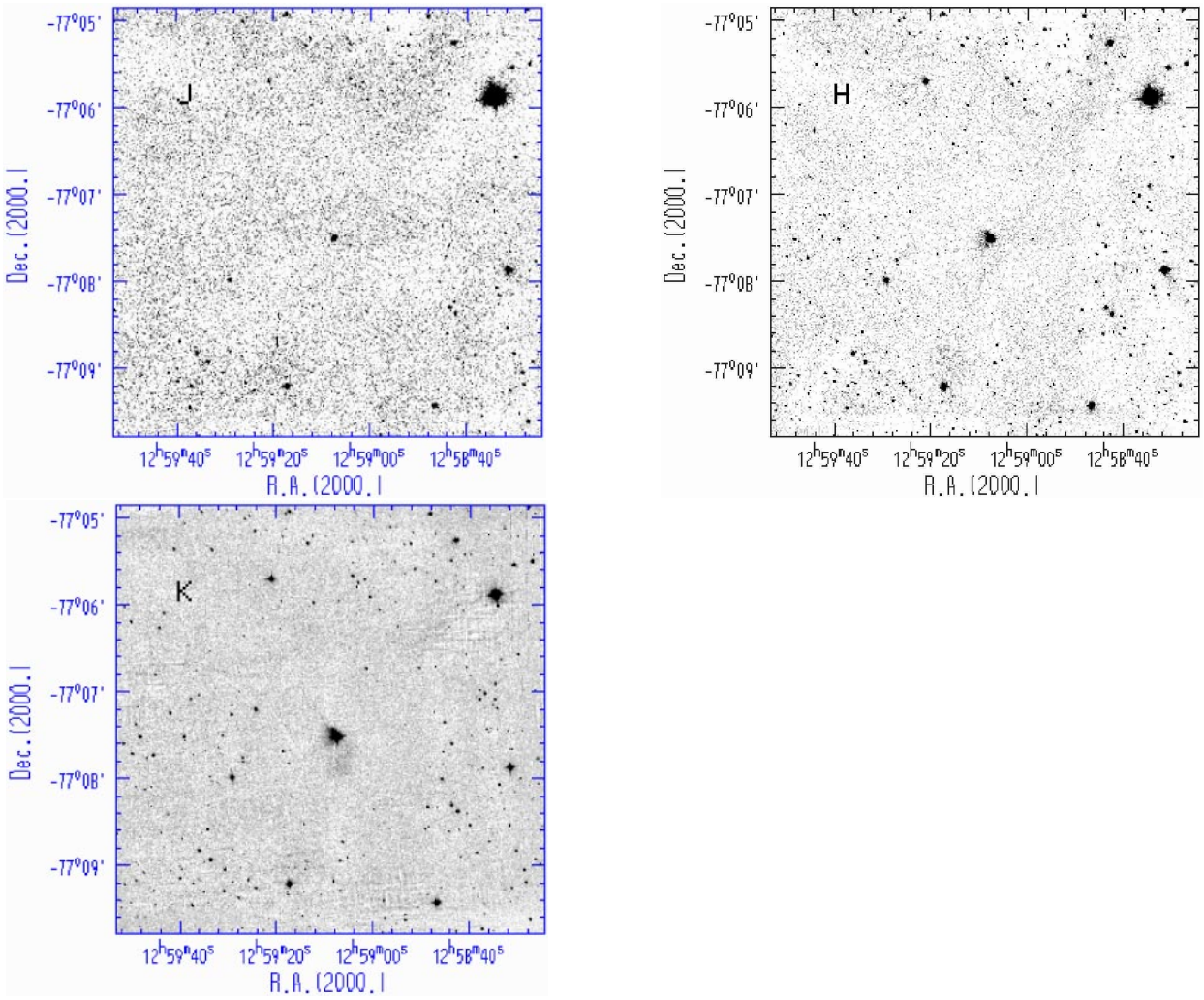

Fig. 1. JHK_s images of Cha II. The central source is IRAS 12553–7651.

3. Discussion

3.1. The nature of the ISOCAM sources

Most of the sources found at 6.75 μm in Cha II (~70% of the sample) have optical counterparts on the DSS plates and have been detected in the near-IR by the DENIS survey. In addition all the previously known members of the cloud lying in our survey region have been detected by ISOCAM.

As discuss by Persi et al. (2000) the analysis of the ISOCAM color-magnitude diagram ($m_{14.3}$ vs. $m_{6.7}-m_{14.3}$) or the color-color plot ($J - K_s$ vs. $K_s-m_{6.7}$) for sources detected only at 6.75 μm is a powerful method to discriminate young objects from field stars in nearby clouds. Figure 3 shows these two diagrams. The left panel plots 32 sources detected in both ISOCAM filters, while the right panel displays 70 objects with LW2 band measurements and near-IR counterparts.

Sources with $m_{6.7}-m_{14.3} \sim 0$ are field stars (open squares) or Class III objects (open circles) for which the mid-IR emission is mainly due to the stellar photosphere. Six objects in Fig. 3 show clear mid-IR excess that indicates the presence of circumstellar material. Of these six sources, five were previously identified as PMS stars (filled circles) in Cha II, while one very faint source (ISO-ChaII13) is a new detection (filled square).

The second plot (righ panel of Fig. 3), constructed combining the ISOCAM and DENIS data (Cambrésy, private communication), is also very useful to separate the effect of intrinsic IR emission excess from the reddening. We consider sources with intrinsic $K_s - m_{6.7}$ excess those lying to the right of the reddening band (dashed line in Fig. 3 right panel), obtained by shifting the reddening line (Rieke & Lebofsky 1985 reddening law) by an amount determined from the photometric errors. All the mid-IR sources, with only one exception, are located to the right of this band. In addition at least four more sources observed only at LW2 (shown with the symbols "×" in the left panel of Fig. 3) and not previously identified lie in this part of the diagram. These objects may be new candidate YSOs of the Cha II cloud. In particular two of these new sources, ISO-ChaII 73 and 98 have been detected with a $S/N \leq 4$ at LW2 (see Table 2). According to the analysis made by Hogg & Turner (1998) for very faint sources, their fluxes at 6.75 μm may be overestimated and consequently a reliable classification is not possible. Measurements at higher S/N are needed for the two candidates.

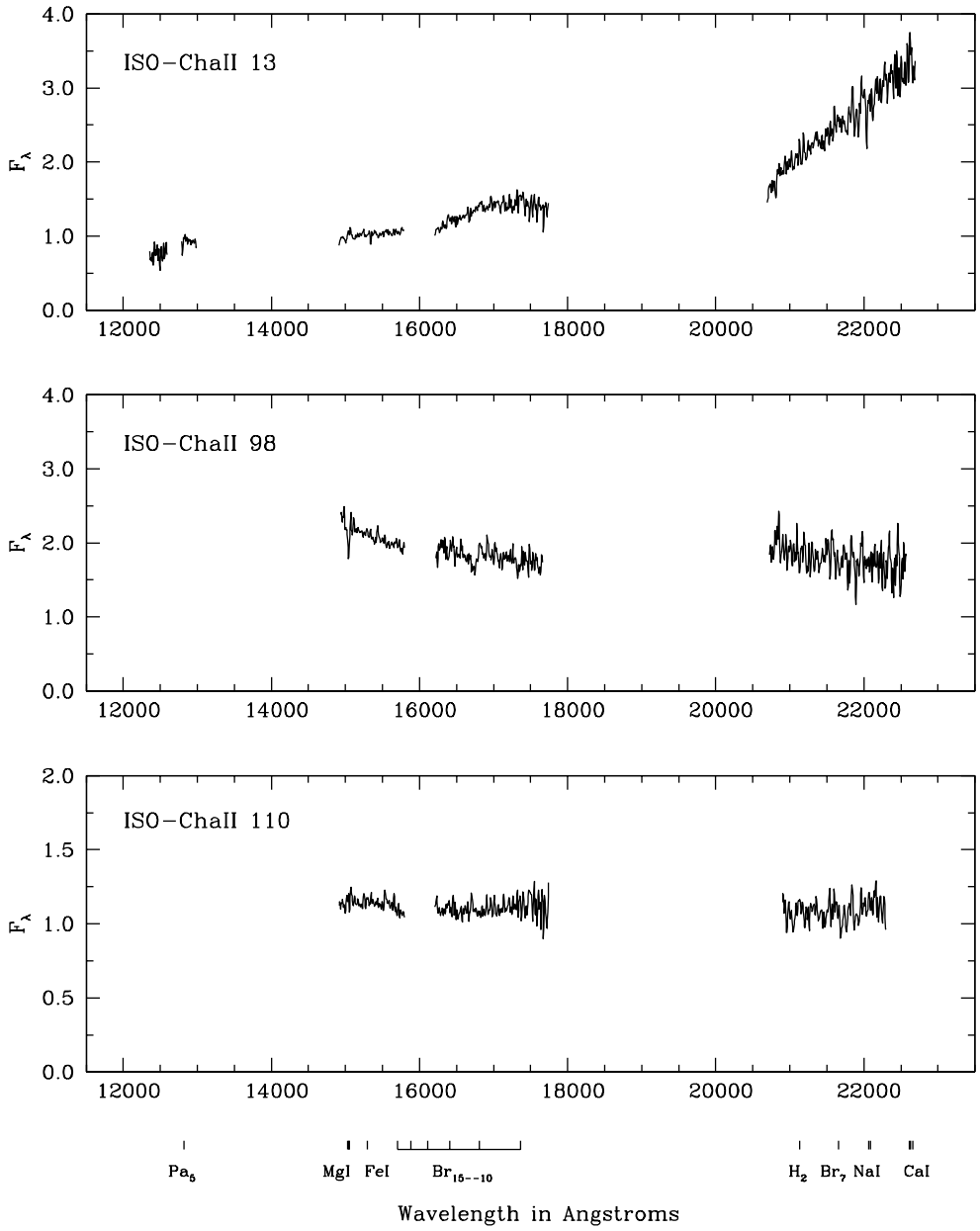

Fig. 2. Near–IR spectra of ISO-ChaII13, 98 and 110.

The location of all the observed ISOCAM sources is superimposed on the optical Digitized Sky Survey (DSS) plate (Fig. 4).

The list of positions, DENIS photometry and ISOCAM flux densities of the previously known members of Cha II, with and without IR excess are reported in Table 3. The DENIS photometric accuracy for these sources is $\leq\pm0.05$ mag. Table 4 provides the same measurements including the 1σ photometric statistical errors for the new candidate YSOs selected from the analysis of Fig. 3. In both tables, the coordinates are taken from the DENIS survey whose accuracy is within $\pm1''$.

We have computed the spectral index $\alpha_{2.2-14.3\,\mu\mathrm{m}} = \mathrm{dlog}\lambda F_\lambda/\mathrm{dlog}\lambda$ and have derived the spectral energy distribution class for each previously known PMS star in the cloud (Cols. 8 and 9 of Table 1). This classification correlates with the evolutionary stage of the low mass stars (Lada 1987). The source IRAS 12553–7651 (ISO-ChaII28), here classified as Class I, is presumably the youngest object observed in Cha II. Its characteristics will be discussed in the next sections.

The newly discovered source ISO-ChaII13 with mid-IR excess is particularly interesting. We have applied the procedure described by Persi et al. (2000) to derive the stellar luminosity of this source. From the J magnitude (see Table 2) and the observed 3σ upper limit magnitude in $I(0.8\,\mu\mathrm{m}) \geq 18$ (Cambrèsy private communication), we obtain $A_J \geq 1.1$ and $L\star \geq 0.01\ L_\odot$. In this estimate we have assumed a distance of 178 pc (Whittet et al. 1997), an intrinsic color $(I-J)_o = 1.5$, and a bolometric correction $BC_J = 1.80$. These values have been obtained from the Kenyon & Hartmann (1995) calibration taking a mean spectral type between M 2.5 and M 6 for the central object. Moreover the integration of the spectral energy distribution from 1 to 14.3 μm gives a similar value

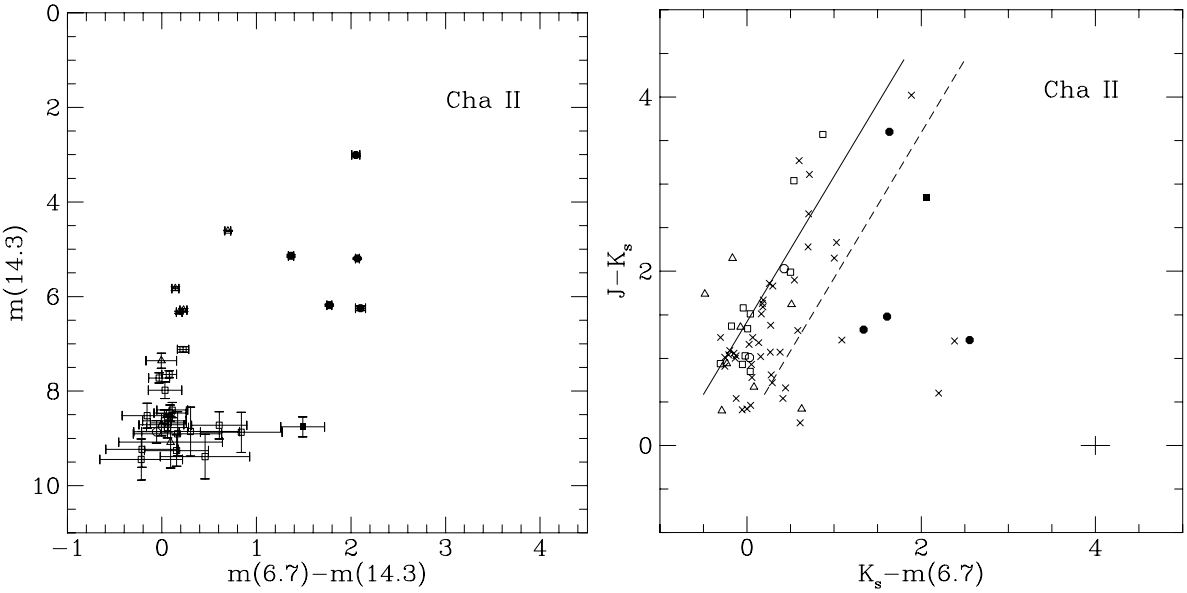

Fig. 3. Color–magnitute (left panel) and color–color (right panel) plots for the ISOCAM sources in Cha II. Filled circles are known PMS stars with mid-IR excess, open circles are known Class III sources without IR excess, open triangles are field stars (Hughes & Hartigan 1992), and open squares are new detections without mid-IR excess. The symbols "×" in the right panel correspond to the sources detected only at LW2, while the filled square is the new candidate PMS source ISO-ChaII13 with mid-IR excess. The cross at the lower right corner of the right panel indicates mean photometric error.

Table 3. ISOCAM and DENIS photometry of the identified sources in Cha II.

ISO-ChaII	α(2000)	δ(2000)	J	K_s	$F_{6.7}$	$F_{14.3}$	α(IR)	Class.	Id.
	h m s	° ′ ″	mag	mag	(mJy)	(mJy)			
28	12 59 07.0	−77 07 39		10.94	792.7(26.3)	1190.1(25.1)	+1.0	I	IRAS12553–7651
29	12 59 10.5	−77 12 13	11.26	9.23	25.1(0.9)	5.4(1.2)	−2.7	III	CHIIXR3
51	13 00 54.8	−77 08 59	11.70	10.50	55.0(0.8)	63.7(1.2)	−0.8	II	Sz48,CHIIXR7
52	13 00 55.5	−77 10 22	10.35	8.87	103.8(1.6)	158.1(1.8)	−1.1	II	Sz50,CHIIXR8
55	13 00 56.4	−76 54 02	8.98	8.03	38.1(0.8)	59.9(2.7)	−1.9	II	Sz49,CHIIXR9
54	13 00 59.5	−77 14 03	11.74	8.14	208.3(3.6)	166.4(3.2)	−1.4	II	CHIIXR10
91	13 02 55.7	−77 15 16	9.86	9.32	13.9(0.7)			III	CHIIXR17
94	13 03 04.7	−77 07 03	9.59	8.58	31.6(0.7)	7.8(1.2)	−2.8	III	CHIIXR18

Table 4. ISOCAM and DENIS photometry of the new candidate YSOs in Cha II.

ISO-ChaII	α(2000)	δ(2000)	J	K_s	$F_{6.7}$	$F_{14.3}$
	h m s	° ′ ″	mag	mag	(mJy)	(mJy)
13	12 58 06.8	−77 09 09	15.15(0.12)	12.30(0.11)	6.7(0.6)	6.0(1.2)
73	13 01 46.2	−77 16 03	13.27(0.09)	12.06(0.11)	3.4(0.7)	
98	13 03 26.2	−77 01 48	14.57(0.13)	13.37(0.16)	3.4(0.9)	
110	13 04 19.2	−77 54 00	13.26(0.08)	12.66(0.12)	5.5(0.8)	

of ∼0.02 $L_\odot$. The derived lower limit of the luminosity of 0.01 $L_\odot$ suggests this source, according to the mass-luminosity relation of D'Antona & Mazzitelli (1998), a young brown dwarf with an age of 1–10 Myr. In order to confirm this result, a more accurate near-IR spectrum of ISO-ChaII13 with higher S/N is required to determine the $T_{\rm eff}$ and a correct classification. In fact the near-IR spectrum of Fig. 2 that shows a rising shape toward wavelengths longer than 2 μm is not suitable for a spectral classification of ISO-ChaII13. This source together with IRAS 12553–7651, lies in the densest part of the cloud (see Fig. 4).

The spectra of the other two candidate YSOs in ChaII (ISO-ChaII 98, and 110) are featureless at the resolution used and have constant flat spectral shapes (Fig. 2).

3.2. The central and densest part of Cha II

High sensitivity and sub-arcsec resolution J, H, and K_s images of the central part of Cha II show a wide region empty of stars, indicating a high value of visual extinction in the core of the dark cloud (see Fig. 1).

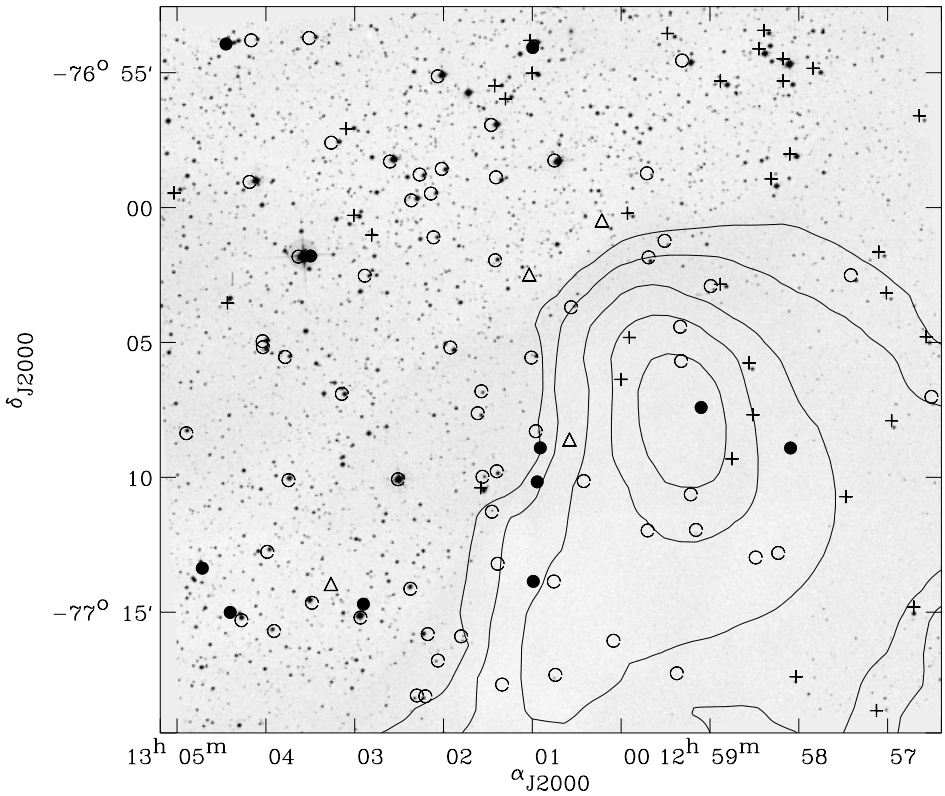

Fig. 4. Spatial distribution of the ISOCAM sources in Cha II superimposed on the DSS plate. The contours represent the extinction map of Vuong et al. (2001). Filled and open circles indicate sources with and without IR excess.

The sources detected in the three filters (103 in total) are shown in the $J - H$ vs. $H - K$ plot of Fig. 5. This diagram allows us to discriminate field reddened stars from YSOs. Most of the sources have colors consistent with reddened background stars with $A_V \sim 10$–15. However at least 10 very faint objects not detected by ISOCAM may have near-IR excesses typical of reddened CTTS. Statistical photometric errors of most of these sources are large and higher precision data are required to confirm these colors excesses. Table 5 gives photometry for these candidate new members of the cloud. The statistical photometric errors are in brackets and where not indicated are $\leq \pm 0.05$ mag. The designation of the sources is the same as in the complete list of Table 2.

ISOCAM detected four sources in the central part of the cloud (ISO-ChaII23, 24, 28, and 31). Three of these objects show no mid- or near-IR excess (see Fig. 5) and thus are probably reddened field stars. On the contrary the fourth source, ISO-ChaII28 (IRAS 12553–7651), has strong near-IR color excesses and moderate photometric errors. We will discuss this object in more detail in the next section.

Figure 6 shows the K vs. $H - K$ diagram for the detections with H and K magnitudes. Sources in Table 5 with likely near-IR excesses are indicated with filled squares and objects without detected color excesses as open squares. Superimposed on this plot are the isochrones for 1 Myr and 10 Myr (solid lines) corresponding to de-reddened low mass stars and brown dwarfs at the distance of the Cha II cloud obtained from D'Antona & Mazzitelli's (1998) model. The reddening lines for $A_V = 10$ mag and for a 0.08 $M_\odot$ object of 1 and 10 Myr,

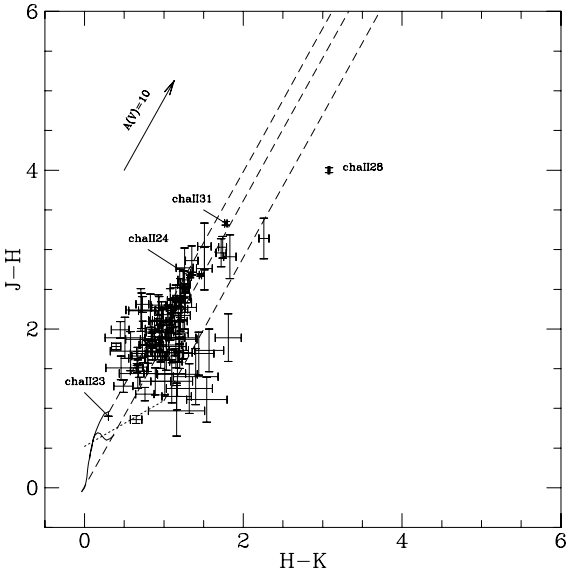

Fig. 5. $J - H$ vs. $H - K$ diagram of 103 sources detected in the central part ($4.9' \times 4.9'$) of Cha II. The solid line marks the loci of the main sequence stars from Bessel & Brett (1988), while the dashed lines define the reddening band extending from the main sequence, using the standard reddening vector from Rieke & Lebofsky (1985). The dotted lines represent the colors of un-reddened classical T Tauri stars (Meyer et al. 1997).

respectively, are shown with dashed lines. Most of the sources lie below the reddening line for objects with mass at the H-burning limit. However, only those belonging to the cloud

Table 5. Coordinates and photometry of the new candidate YSOs in the core of Cha II.

NIR	α(2000)	δ(2000)	J	H	K_s
	h m s	° ′ ″	mag	mag	mag
20	12 58 31.50	−77 09 42.7	21.06(0.22)	20.09(0.23)	18.93(0.27)
56	12 58 41.68	−77 08 53.8	20.82(0.23)	19.13(0.14)	17.69(0.13)
71	12 58 46.91	−77 05 43.9	20.89(0.23)	19.16(0.14)	17.59(0.12)
91	12 58 54.86	−77 06 14.2	20.85(0.24)	19.60(0.20)	18.28(0.21)
104	12 59 04.16	−77 05 16.1	18.01	17.15	16.50(0.06)
110	12 59 07.40	−77 07 30.9	17.87	13.87	10.79
114	12 59 13.17	−77 09 42.4	20.84(0.21)	19.73(0.19)	18.19(0.17)
132	12 59 22.50	−77 09 44.8	21.22(0.29)	19.82(0.20)	18.42(0.20)
183	12 59 47.02	−77 08 07.4	20.92(0.27)	19.03(0.13)	17.22(0.10)
185	12 59 47.40	−77 09 04.6	20.01(0.12)	18.86(0.12)	17.70(0.14)
186	12 59 48.05	−77 07 30.9	20.91(0.25)	17.77	15.51

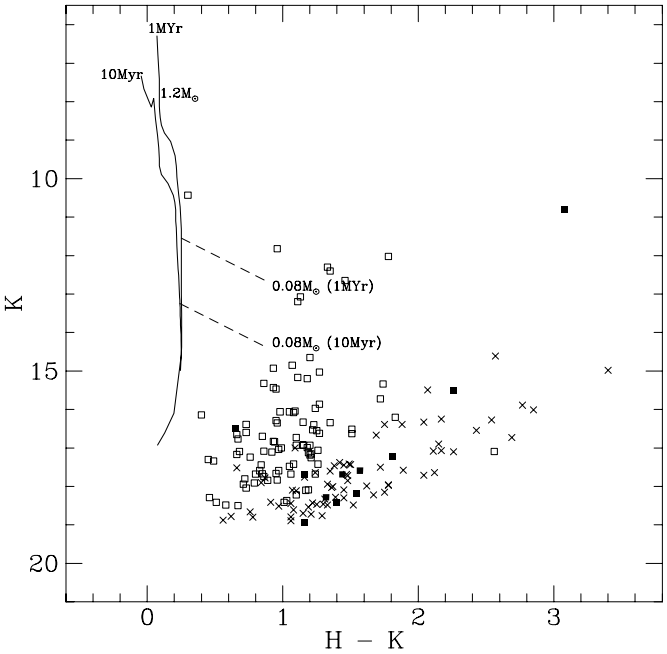

Fig. 6. K vs. $H-K$ diagram of the sources in Cha II. The solid lines indicate the 1 Myr and 10 Myr isochrones for low mass stars and brown dwarfs from the models of D'Antona & Mazzitelli (1998). Reddening lines for A_V = 10 mag (dashed lines) are drawn for a 0.08 $M_\odot$ object of 1 and 10 Myr, respectively. Filled and open squares represent sources with and without IR excess, while crosses are sources not detected in J.

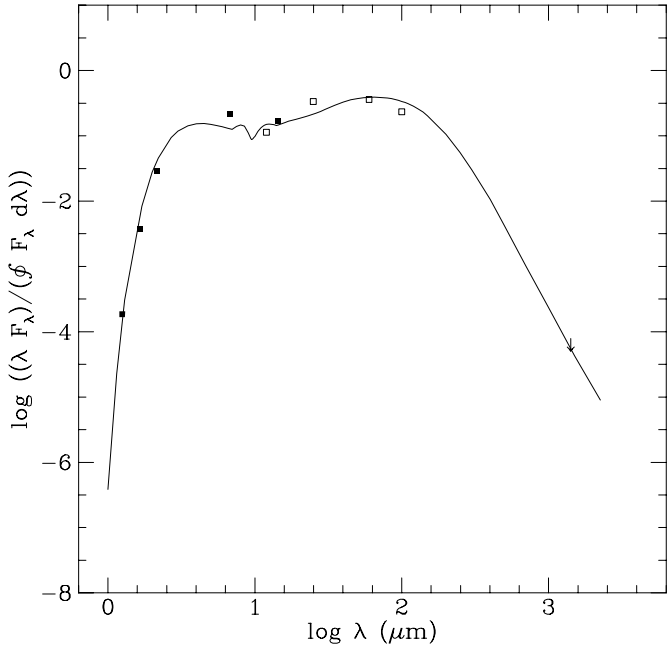

Fig. 7. The spectral energy distribution of IRAS 12553–7651 (ISO-ChaII28). Filled squares correspond to our near and mid-IR observations, while open squares are IRAS data. The arrow indicates the 1.3 mm upper limit (Henning et al. 1993). The solid line is the spherically symmetric model obtained from the DUSTY code.

(i.e., having near-IR color excesses) are likely reddened young brown dwarf members of the cloud. We caution, however, that higher signal to noise ratio photometry in combination with near-IR spectroscopy are needed to confirm the sub-stellar nature of these very faint sources (see Table 5) found in the Chamaeleon II dark cloud. Objects with similar characteristics to these Cha II extremely low luminosity sources have been detected in other nearby clouds. In particular several have been found in Chamaeleon I (Neuhäuser & Comerón 1999; Comerón et al. 1999; Persi et al. 2000). The existence of sub-stellar objects in nearby star-forming regions seems to be a common phenomenon.

3.2.1. IRAS 12553–7651(ISO-ChaII28)

We have classified IRAS 12553–7651 as a Class I member of the cloud based on the spectral index α as discussed in Sect. 3.1. (see Table 3). This source lies at the center of the densest region of the cloud (see Figs. 1 and 4) and it is associated with a small nebulae at 2.2 μm (see Fig. 1). We combined near-IR photometry of Table 2, the ISOCAM flux densities of Table 3 and the IRAS data with the 1.3 mm upper limit obtained by Henning et al. (1993). Figure 7 shows the spectral energy distribution (SED) for this object. This SED rises from 1 to 2 μm, is roughly flat in the 2–100 μm interval and then falls off at longer wavelengths. Integrating the SED we derived a bolometric luminosity $L_{\rm bol}$ of 1.49 $L_\odot$ for this object.

Table 6. Model parameters of IRAS 12553–7651 derived from the DUSTY code.

T_e	4000 K
T_i	1300 K
A_V	50
F_{Tot}	1.5×10^{-16} W/cm^2
r_i	2.4×10^{12} cm
r_o	2.4×10^{16} cm
T_d	17 K

We adopt a spherically symmetric dust envelope model (Ivezić & Elitzur 1997) developed by the DUSTY code (Ivezić et al. 1999) to fit the SED of IRAS 12553–7651. We assume standard optical properties for the dust grains (Draine & Lee 1984), a density distribution of the type $n(r) \propto r^{-0.8}$, a temperature for the central star $T_e = 4000$ K, and a temperature at the inner radius $T_i = 1300$ K. Table 6 summaries the derived parameters and the solid line in Fig. 7 reproduces the fitted model. The model parameters include r_i and r_o, the inner and outer radii of the envelope and T_d, the dust temperature at r_o. The high value of the optical extinction in Table 6 ($A_V = 50$) indicates that this object is deeply embedded in the core of the Cha II cloud.

4. Conclusions

An area of 28′×26′ of the Cha II has been surveyed at 6.75 and 14.3 μm with ISOCAM. Sub-arcsec resolution JHK_s images have been obtained for the central $4.9' \times 4.9'$ of the cloud. The analysis of these mid- and near-IR images in combination with the DENIS data in the cloud allow us to reach the following conclusions:

1) A total of 115 point sources with $S/N \geq 3$ have been detected with ISOCAM, of which 112 are at 6.75 μm and 35 are at 14.3 μm. A small number of these sources show a mid-IR excess and/or 2.2–6.75 μm excess emission. Most of these objects are previously known PMS stars of the cloud. We classify them using the observed infrared spectral index.

2) Only one Class I source (ISO-ChaII28) identified with IRAS 12553-7651 is located in the region. This YSO has a bolometric luminosity $L_{bol} = 1.49\ L_\odot$ and is deeply embedded ($A_V = 50$) in the central part of Cha II. In addition it shows a very faint nebulosity at 2.2 μm.

3) In the same central area, ISOCAM has detected a new source (ISO-ChaII13) with mid-IR excess. The derived stellar luminosity ($\geq 0.01\ L_\odot$) suggests the presence of a sub–stellar object at the distance of the cloud. The near-IR spectrum of ISO-ChaII13 appears featureless at our spectral resolution with a raising spectral shape at $\lambda \geq 2$ μm.

4) The analysis of the $J - H$ vs. $H - K$ diagram of the sources detected in the central part of the Cha II (see Fig. 5) shows approximately ten objects with near-IR excess. These sources are located well below the loci of sub-stellar objects with ages between 1 and 10 Myr in the color-magnitude (K vs. $H - K$) diagram. However these deeply embedded objects are very faint and the corresponding magnitudes and colors have large uncertainties. Higher S/N photometry and near-IR spectroscopy are required to confirm this result.

Acknowledgements. We are grateful to L. Cambrésy for providing the DENIS data.

References

Alcalá, J. M., Covino, E., Sterzik, M. F., et al. 2000, A&A, 355, 629
Bessel, M. S., & Brett, J. M. 1988, PASP, 100, 1134
Bontemps, S., André, P., Kaas, A. A., et al. 2001, A&A, 372, 173
Boulanger, F., Bronfman, L., Dame, T. M., & Thaddeus, P. 1998, A&A, 332, 273
Cesarsky, C. J., Abergel, A., Agne'se, P., et al. 1996, A&A, 315, L32
Comerón, F., Rieke, G. H., & Neuhauser, R. 1999, A&A, 343, 477
D'Antona, F., & Mazzitelli, I. 1998, Mem. Soc. Astron. It., 68, 807
Draine, B. T., & Lee, H. M. 1984, ApJ, 285, 89
Gómez, M., & Persi, P. 2002, A&A, 389, 494
Hartigan, P. 1993, AJ, 105, 1511
Henning, Th., Pfau, W., Zinnecker, H., & Prusti, T. 1993, A&A, 276, 129
Hogg, D. W., & Turner, E. L. 1998, PASP, 110, 727
Hughes, J., & Hartigan, P. 1992, AJ, 104, 680
Kaas, A. A., Olofsson, G., Bontemps, S., et al. 1999, in The Universe as seen by ISO, ESA SP-427, 493
Kenyon, S. J., & Hartmann, L. 1995, ApJS, 101, 117
Kessler, M. F., Steinz, J. A., Anderegg, M. E., et al. 1996, A&A, 315, L27
Ivezić, Z., & Elitzur, M. 1997, MNRAS, 287, 799
Ivezić, Z., Nenkova, M., & Elitzur, M. 1999, User Manual for Dusty (University of Kentucky), Internal Report
Lada, C. J. 1987, in Star Forming Regions, IAU 115, 1
Larson, K. A., Whittet, D. C. B., Prusti, T., & Chiar, J. E. 1998, A&A, 337, 465
Meyer, M. R., Calvet, N., & Hillebrand, L. A. 1997, AJ, 114, 288
Neuhäuser, R., & Comerón, F. 1999, A&A, 350, 612
Nordh, L., Olofsson, G., Abergel, A., et al. 1996, A&A, 315, L185
Olmi, L., Felli, M., & Prusti, T. 1994, A&A, 288, 591
Olmi, L., Felli, M., & Cesaroni, R. 1997, A&A, 326, 373
Olofsson, G., Huldtgren, M., Kaas, A. A., et al. 1999, A&A, 350, 883
Persi, P., Marenzi, A. R., Kaas, A. A., et al. 1999, AJ, 117, 445
Persi, P., Marenzi, A. R., Olofsson, G., et al. 2000, A&A, 357, 219
Persi, P., Marenzi, A. R., Gómez, M., & Olofsson, G. 2001, A&A, 376, 907
Persson, S. E., Murphy, D. C., Kreminsky, W., et al. 1998, AJ, 116, 2475
Prusti, T., Whittet, D. C. B., Assendorp, R., & Wesselius, P. R. 1992, A&A, 260, 151
Rieke, G. K., & Lebofsky, M. J. 1985, ApJ, 288, 618
Schwartz, R. D. 1977, ApJS, 35, 161
Stetson, P. B. 1987, PASP, 99, 191
Vuong, M. H. L., & Epchtein, N. 2001, A&A, 379, 208
Whittet, D. C. B., Assendorp, R., Prusti, T., et al. 1991, A&A, 251, 524
Whittet, D. C. B., Prusti, T., Franco, G. A. P., et al. 1997, A&A, 327, 1194